

# Analysis of the anisotropic light scattering spectrum in liquids

L. A. Zubkov, N. B. Rozhdestvenskaya, and V. P. Romanov

A. A. Zhdanov Leningrad State University

(Submitted April 28, 1973)

Zh. Eksp. Teor. Fiz. 65, 1782-1796 (November 1973)

Angular measurements of the spectra of the  $I_{xy}^z$  component of anisotropic light scattering have been carried out in quinoline. The phenomenological parameters involved in the hydrodynamic theory of anisotropic scattering in the presence of two relaxation processes are determined by analyzing the scattering spectra and the measurements of the Maxwell constant. The theoretical spectra are calculated with the aid of these data and are then modified by the apparatus function of the optical system. They are then compared with the experimental spectra. Quantitative agreement is observed between theory and experiment. For strong spacing of the relaxation times which are observed, the central part of the  $I_{xy}^z$  component spectrum and the Maxwell constant are practically completely due to the anisotropy tensor, which possesses the larger characteristic time. The contribution of orientations to the shear viscosity is determined by comparing the results with molecular theories. It is shown that reorientation of molecules is of an individual nature to a large extent.

The study of the interaction of electromagnetic radiation with matter in the optical frequency range is today one of the most important methods for obtaining information on the structure and kinetic properties of liquids. Great interest attaches to the spectral composition of that depolarized part of the scattered light, for the appearance of which the anisotropic fluctuations are responsible. When the incident radiation propagates along the x axis and is observed in the xy plane, the spectra of the  $I_{xy}^z$  and  $I_{xy}^y$  components are completely different. Here the superscript denotes the direction of polarization of the incident light and the subscript that of the scattered light.

The presence of two peaks in the intensity at the Mandel'shtam-Brillouin frequency, discovered by Stegeman and Stoicheff, is a distinguishing feature of the structure of the  $I_{xy}^y$  contour.<sup>[1]</sup> The fine structure of the  $I_{xy}^z$  component was first observed by Starunov, Tiganov and Fabelinskii,<sup>[2]</sup> and then by Stegeman and Stoicheff.<sup>[1]</sup> Further investigations showed that a broad, Lorentzian line is additionally present in the spectra of both components.<sup>[3,4]</sup> Neither the shape of the spectrum nor its angular and temperature dependences are described by the simple phenomenological theory of Leontovich.<sup>[5]</sup> For the explanation of the observed behavior, a generalization of the Leontovich theory has been carried out for the case of an arbitrary number of tensor and scalar relaxation variables.<sup>[6,7]</sup> It has been possible to explain qualitatively almost all the features of the observed scattering spectra within the framework of such a generalized model. However, serious difficulties develop in the quantitative comparison, because many parameters that must be obtained from experiments remain unknown, and very arbitrary assumptions must be made on their values.<sup>[5-7]</sup>

Along with the phenomenological theory, there are also molecular theories of the depolarized light scattering.<sup>[8-12]</sup> At the base of these theories lies the assumption that the narrower Lorentzian line is connected with processes of reorientation of the molecules. The fine structure in the lines arises because of the interaction of the field of the orientations with longitudinal and transverse acoustic modes. The experimental study of the fine structure parameters is most essential to test the validity of the molecular theories, since the theories are most sensitive to them.

In the present paper, the spectrum of anisotropic

light scattering has been studied in detail in a pure liquid and in solutions. The characteristics of the spectra have been determined and their dependence on the scattering angle and on the temperature have been investigated. The quantities that enter into the microscopic theory have been calculated on the basis of these data and certain conclusions have been drawn on the character of the process of molecular reorientation.

For quinoline, all the parameters of the phenomenological theory of anisotropically scattered light have been determined and a comparison made of the theoretically constructed spectra with the experimental ones.

## 1. THE EXPERIMENTAL SETUP AND THE METHOD OF TREATMENT OF THE RESULTS OF MEASUREMENT

Figure 1 shows the setup of the apparatus on which the study of the angular dependence of the  $I_{xy}^z$  and  $I_{xy}^y$  components of the scattered light in quinoline were carried out. We used an LG-36A He-Ne laser as the light source (the half-width of the apparatus function was  $2\Delta\nu_A = 0.025-0.30 \text{ cm}^{-1}$  at a spectral apparatus dispersion  $\nu_D = 0.5 \text{ cm}^{-1}$ ), and also the single-frequency laser LG-159 ( $2\Delta\nu_A = 0.011 \text{ cm}^{-1}$ ). The scattering angle was varied by rotating the mirror  $M_1$  and moving it along the axis of the laser. All the other units of the apparatus remained immobile. The scattering angles were established accurate to  $1.5^\circ$  in the range from  $30$  to  $150^\circ$ .

A photoelectric recording method was used, employing a Fabry-Perot etalon, which scanned the spectrum by varying the air pressure in the pressure chamber of the etalon. Light passing through a diaphragm  $D_3$  of diameter  $\approx 0.3 \text{ mm}$ , which was located in the focal plane of the objective  $L_3$ , fell on the photocathode of a cooled FEU-79 photomultiplier operating in a pulse-counting regime. The cooling apparatus for the photomultiplier is shown in Fig. 2. The cooling element was a semiconductor microrefrigerator, fed by a current of 30 A from a VSP-22 source. The temperature in the microrefrigerator reached  $-27^\circ\text{C}$  within one hour after cooling with running water was switched on. The electric pulses were recorded by the linear rate meter PI-4-1. The number of recorded pulses in our experiment with the LG-36A did not exceed 2000/sec. With the light source LG-159, the useful signal did not exceed 200 counts/sec

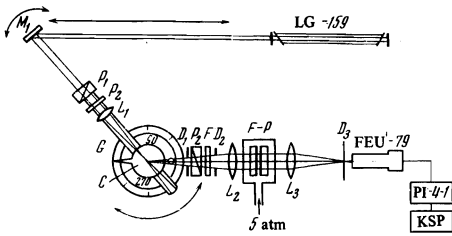


FIG. 1. Schematic arrangement for angular measurements of the spectra of scattered light: LG-159 – single-frequency He-Ne laser;  $M_1$  – rotatable mirror;  $P_1, P_3$  – Frank – Ritter prisms,  $P_2$  – half-wave plate;  $G$  – goniometer;  $C$  – cell;  $D_1, D_2, D_3$  – diaphragms;  $F$  – filter;  $L_1, L_2, L_3$  – lenses;  $F-P$  – Fabry-Perot etalon in pressure chamber; FEU-79 – photomultiplier with exit diameter  $\approx 0.3$  mm; PI-4-1 – linear analog intensity meter, KSP – recording unit.

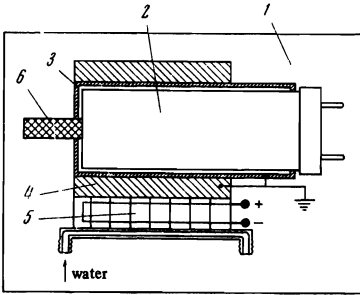


FIG. 2

FIG. 2. System for cooling the photomultiplier: 1 – foamed plastic case, 2 – FEU-79 photomultiplier 3 – aluminum container; 4 – copper ring with ground connection; 5 – miniature refrigerator; 6 – plastic rod.

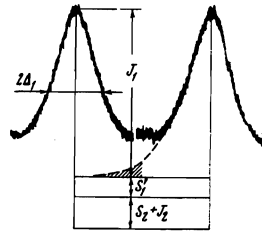


FIG. 3

FIG. 3. Spectrum of the  $I_{xy}$  component for two neighboring orders of the Fabry-Perot etalon.  $J_1$  – amplitude of the  $L_1$  line of given order,  $S_1'$  – amplitude of the contributions from the  $L_1$  lines of all orders except the zeroth;  $S_2 + J_2$  – amplitude of the contributions of all  $L_2$  lines. The shaded region is the contribution from  $n = \pm 1$ , which distorts the shape of the spectrum.

and the dark current of the cooled photomultiplier was 8–12 counts/sec. The temperature of the liquid in the cylindrical cell  $C$  was kept constant to within  $\pm 0.5^\circ$  by a “Vobser” thermostat.

As has been shown previously,<sup>[13]</sup> the spectrum of the  $I_{xy}^z$  components can be represented as the superposition of three Lorentzians: two positive,  $L_1$  and  $L_2$ , with sharply differing half-widths  $\Delta_1 \ll \Delta_2$ , and a single Lorentzian line  $L_{neg}$  in the central part of the spectrum. From this spectrum we can, in principle, determine both half-widths of the positive Lorentzian contours, the ratio of their intensities, and also the relative depth of the dip.

Inasmuch as the central dip distorts the half-width of the  $L_1$  dispersion contour, it is more accurate to use the spectrum of the  $I_{xy}^y$  component in its determination; this component is obtained at the scattering angle  $\theta = \pi/2$ . At this angle, the component consists of the contours  $L_1$  and  $L_2$  and a weak doublet<sup>[1]</sup> at the Mandel'shtam-Brillouin frequency  $\Omega_B$ . The temperature of  $11^\circ C$  was chosen from the consideration that  $\Omega_B > \Delta_1$  here, and, as is seen from Fig. 3, the Mandel'shtam-Brillouin doublet does not distort the contour  $L_1$  at the frequency  $\Delta_1$ .

The half-width of the contour  $L_1$  was found from the spectrum by means of the method of successive approximations, similar to what was described in<sup>[14]</sup>. The

half-width of the contour  $L_2$  is usually larger than or of the order of  $5 \text{ cm}^{-1}$ , which far exceeds the range of dispersion of the interferometer; therefore, the spectrum of the contour  $L_2$ , recorded on our apparatus, represents a straight line. To estimate the half-width of this line, we used the spectrum obtained on apparatus in which a DFS-12 spectrograph was used as the spectral instrument.

In the calculation of the ratio of the integrated intensities of the contours  $L_1$  and  $L_2$ , it is necessary to take it into account that the spectrum of given order ( $n = 0$ ) is composed of two Lorentzian curves

$$L_1 = \frac{J_1}{1 + \nu^2/\Delta_1^2}, \quad L_2 = \frac{J_2}{1 + \nu^2/\Delta_2^2}$$

with the maxima in the middle of this spectrum, and sums of the contributions

$$S_1(\nu) = \sum_{n > |n| > 1} J_1^{(n)} / \left[ 1 + \left( \frac{\nu + n\nu_D}{\Delta_1} \right)^2 \right]$$

and

$$S_2(\nu) = \sum_{n > |n| > 1} J_2^{(n)} / \left[ 1 + \left( \frac{\nu + n\nu_D}{\Delta_2} \right)^2 \right]$$

of the spectra of all the remaining orders (Fig. 3). Inasmuch as the dispersion range of the interferometer  $\nu_D$  is such that  $\Delta_2/\nu_D \gg 1$ , the quantities  $L_2$  and  $S_2$  are practically independent of the frequency within the limits of a single order. Recognizing that in Fabry-Perot interferometers with photoelectric recording by the scanning method all the amplitudes  $J^{(n)}$  are independent of the number of the spectrum, we get the result that the area

$$\nu_D (J_2 + S_2) = \sum_{n=-\infty}^{+\infty} \frac{J_2 \nu_D}{1 + (n\nu_D/\Delta_2)^2} \approx \int_{-\infty}^{+\infty} \frac{J_2 d\nu}{1 + (\nu/\Delta_2)^2}$$

for the spectrum of each order is equal to the integrated intensity of the line  $L_2$ .

So far as the quantity  $S_1(\nu)$  is concerned, the contribution to it from those parts of the orders  $n = \pm 1$  which distort the shape of the spectrum, is taken into account directly. The remaining contribution and the contributions of the more distant orders  $S_1'$  can be assumed to be independent of  $\nu$  in the limits of the range of dispersion; it is calculated from the known  $\Delta_1$  and  $J_1$  by direct summation. The area  $S_1' \nu_D + s'$ , as also in the case  $S_2$ , makes the integrated intensity of the line  $L_1$  complete.

Thus the ratio of the integrated intensities of the two lines is equal to

$$(I_1 + s' + \nu_D S_1') / [\nu_D (S_2 + J_2)],$$

where

$$I_1 = \int_{-\nu_D/2}^{+\nu_D/2} \frac{J_1 d\nu}{1 + (\nu/\Delta_1)^2}$$

and is determined by planimetry of the spectra. The accuracy of the determination of these quantities is of the order of 15%, and is limited by the fact that the high-frequency part of the wing of the Rayleigh line also makes a contribution to the line  $L_2$  and this is difficult to take into account.

To obtain the relative depth of the dip, the spectrum of the  $I_{xy}^z$  component was augmented until the purely dispersion component with halfwidth  $\Delta_1$ , obtained from the spectrum of the  $I_{xy}^y$  component was obtained. For

this purpose, we estimated the position of the null line of the  $L_1$  contour from the overlap of the spectra. Then the level of the null line was varied with the aid of plots of  $1/J(\nu)$  against  $\nu^2$ , where  $J(\nu)$  is the amplitude of the spectrum, until best agreement of the half-width of the constructed contour with  $\Delta_1$  is obtained. The experimental value was then subtracted from this contour. At the temperature of the experiment (11°C), the difference contour is itself a Lorentzian curve.  $\Delta_{\text{neg}}$  and the  $J_{\text{neg}}(0)$  obtained from it differ from the real value because of the apparatus function. The apparatus function was approximated by the Voigt function and separated by the method suggested in<sup>[15]</sup>.

## 2. COMPARISON OF THE RESULTS OF MEASUREMENT WITH THE MOLECULAR THEORIES

The use of single-frequency lasers makes it possible to increase the resolution and obtain higher quality spectra of the scattered light in the low frequency range. For illustration, we have given the central part of the spectrum of the  $I_{xy}^z$  component, taken in quinoline at the scattering angle  $\theta = 60^\circ$  with a multimode (Fig. 4a) and a single-mode (Fig. 4b) laser. It is seen from a comparison of the drawings that the details of the fine structure are much more distinguishable in the second case. Such measurements are necessary for comparison with molecular theories based on the reorientation of the molecules. The existence of a second, more rapid relaxation process, and also its effect on the fine structure, is in no way taken into account in them. Therefore, for a comparison with these theories, it suffices to investigate only the low-frequency part of the spectrum. For definiteness, we make use of the results of the work of Keyes and Kivelson<sup>[9,10]</sup>. In this research, the fluctuations of the dielectric tensor are considered; these are determined by a dynamic variable—the density of the molecular reorientations. In addition to the primary variable, the density of the curl of the momentum also enters into the linear equation of motion. This quantity causes the interaction of the orientations with the shear modes. This theory gives the following for the spectral component  $I_{xy}^z(\omega)$  at small  $\omega$ :

$$I_{xy}^z(\omega) \sim L_1(\omega) - L_{\text{neg}}(\omega) \sim \frac{\Gamma}{\omega^2 + \Gamma^2} - \frac{\cos^2(\theta/2) R}{\omega^2 + (k^2 \eta / \rho)^2} \frac{k^4 \eta^2}{\rho^2 \Gamma^2}$$

where  $1/\Gamma$  is the time of reorientation relaxation,  $k = (4\pi n/\lambda) \sin(\theta/2)$  is the wave vector of the scattering fluctuation wave,  $n$  is the index of refraction,  $\eta$  is the shear viscosity,  $R$  is the relative contribution made to the viscosity by the orientations. We note that the formulas of Keyes and Kivelson are easily obtained

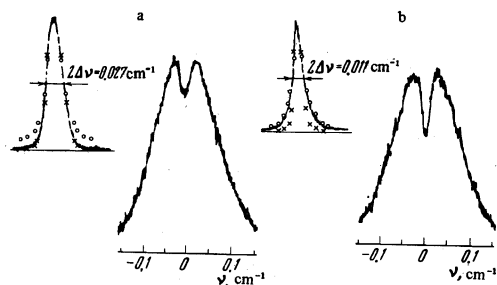


FIG. 4. Apparatus function and spectrum of the  $I_{xy}^z$  component in quinoline ( $\theta = 60^\circ$ ) with multimode laser LG-36A (a) and single-frequency laser LG-159 (b). Lorentzian (O) and Gaussian (X) distribution of the intensity are shown on the spectra of the apparatus functions.

from the Leontovich theory if we assume that only that part of the shear viscosity relaxes which has the characteristic time  $1/\Gamma$ .<sup>[16]</sup> It is seen from the formula for  $I_{xy}^z$  that the neighboring part of the spectrum represents the difference of the two Lorentz contours, as is confirmed by experiment.<sup>[13]</sup> Such a splitting of the  $I_{xy}^z$  component is very convenient for the treatment of the experimental spectra. The value predicted for the half-width of the negative contour,  $\Delta_{\text{neg}} = k^2 \eta / 2\pi\rho$ , admits of direct confirmation Table I gives the values of  $\Delta_{\text{neg}}$  as a function of viscosity for different temperatures. It is seen from the table that the experimental and theoretical values are in agreement within the limits of experimental error. The dependence of  $\Delta_{\text{neg}}$  on  $k^2$  is shown in Fig. 5.

The contribution of the orientations to the shear viscosity can be determined by two methods: from the relative depth of the central dip

$$R = \frac{1}{\cos^2(\theta/2)} \frac{L_{\text{neg}}(0)}{L_1(0)}$$

with subsequent averaging over all the scattering angles and over the separation of the fine-structure components

$$R = (2\nu_{\text{max}})^4 / \left( \Delta_{\text{neg}} \Gamma \cos \frac{\theta}{2} \right)^2$$

In the first case,  $R \approx 0.75$  and in the second,  $R \approx 0.60$ . This divergence is evidently connected with the complexity of an accurate determination of  $\nu_{\text{max}}$  by experiment:  $\nu_{\text{max}}$  enters into the expression for  $T$  in the fourth power.

In a number of researches,<sup>[9,10]</sup> the assumption has been made that the process of reorientation of the molecules in the optical experiments can be described by the simple Debye formula  $\Delta_1 \sim k_B T / \eta a^3$ , where  $a$  is the characteristic dimension of the molecules. However, the validity of such an assumption is not obvious a priori, inasmuch as the molecular reorientations are considered as collective modes in the description of the depolarization spectrum and not as the turnings of individual molecules. Moreover, estimates show that, in quinoline for example, pair correlations of the orientations significantly affect the integrated intensities of the contours  $I_{xy}^y$  and  $I_{xy}^y$ .<sup>[8]</sup> It is possible that this correlation can also affect kinetic processes.

For the elucidation of the reorientation mechanism, we investigated the spectra of anisotropic scattering in solutions of quinoline in neutral solvents: benzene and carbon tetrachloride. The study of solutions is convenient in that it allows us to change the degree of correlation of orientations of the studied material. Inasmuch as the relaxation times of the anisotropy of  $\text{CCl}_4$  and benzene are much smaller, we can track the behavior of the quinoline molecules separately in these mixtures. Figure 6 shows the dependence of the orientation relaxation frequency on the parameter  $T/\eta$ . It is seen from the drawing that the deviation from the dependence  $\Delta_1 \sim T/\eta$  both for mixtures and for pure quinoline does

TABLE I

$t, ^\circ\text{C}$	$\Delta_{\text{neg}, -1} \cdot 10^{-3} \frac{\text{cm}}{\text{experiment}}$	$\Delta_{\text{neg}, \text{calculated}} \cdot 10^{-3} \text{cm}^{-1}$
11	44 ± 1.0	12.5
22	8.7 ± 1.0	9.5
49	5.1 ± 0.7	5.0

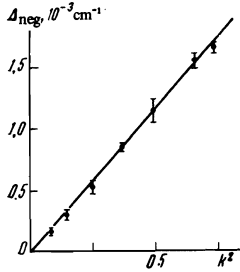


FIG. 5

FIG. 5. Dependence of the half-widths of the negative line on  $k^2 \approx \sin^2(\theta/2)$  with change in the scattering angle  $\theta$ .

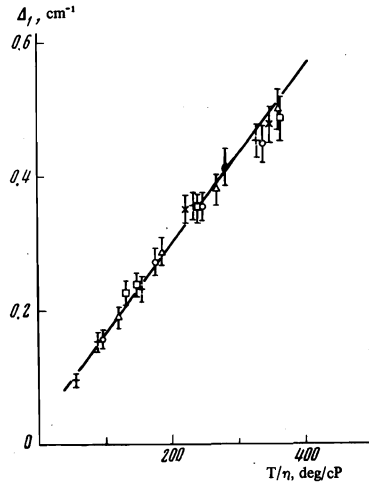


FIG. 6

FIG. 6. Graph of the dependence of the half-width of the line  $L_1$  on  $T/\eta$ . The solid line is for pure quinoline. The points correspond to various concentrations of quinoline in  $CCl_4$  (in mole fractions):  $+$  - 1.0;  $\circ$  - 0.9;  $\Delta$  - 0.8;  $\square$  - 0.6;  $\times$  - 0.3;  $\bullet$  - 0.1.

not exceed 10%. It follows from this that the process of reorientation of the molecules has an individual character to a significant degree and can be described as the hydrodynamic process of the turning of the molecules in a viscous medium. It is interesting to note that when mixtures of various concentration are referred to the same value of  $T/\eta$ , the width of the orientation contour does not change and the fine structure, for example in the case of benzene, disappears at about 0.8 mole fraction of quinoline.

### 3. CALCULATION OF THE PARAMETERS OF THE PHENOMENOLOGICAL THEORY

As a whole phenomenological theories, in contrast to the molecular, describe the entire spectrum of anisotropic scattering. In our specific case, this will be a theory with two internal relaxation processes. In this case, the scattering intensities of interest to us, in the notation of [7], which we shall investigate below, are equal to

$$I_{xy}(\theta) = I_z^y(\theta) \sim \langle (A_1 \zeta_{12}^{(1)} + A_2 \zeta_{12}^{(2)})^2 \rangle_{\omega k} \cos^2 \frac{\theta}{2} + \quad (1)$$

$$+ \langle A_1^2 X_1^2 + A_2^2 X_2^2 \rangle_{\omega k} \sin^2 \frac{\theta}{2}, \quad (2)$$

$$I_{xy}^y(\theta = \pi/2) \sim \langle (A_1 \Phi_1 + A_2 \Phi_2)^2 \rangle_{\omega k} + \langle A_1^2 X_1^2 + A_2^2 X_2^2 \rangle_{\omega k},$$

where  $\zeta_{12}^{(\alpha)}$ ,  $X_\alpha = \frac{1}{2}(\zeta_{22}^{(\alpha)} - \zeta_{33}^{(\alpha)})$  and  $\Phi_\alpha = \zeta_{11}^{(\alpha)}$  are the components of the anisotropy tensor  $\xi_{ik}^{(\alpha)}$  ( $\xi_{ij}^{(\alpha)} = 0$ , the  $x_1$  axis coincides with the direction of the wave vector of the scattering fluctuation wave,  $x_2 \perp x_1$  lies in the  $xy$  plane, and the  $x_3$  axis coincides with the  $z$  axis. The coefficients  $A_\alpha$  determine the dependence of the dielectric constant  $\epsilon$  on  $\zeta_{ik}^{(\alpha)}$ :

$$\delta \epsilon_{ik} = \sum_{\alpha} A_{\alpha} \zeta_{ik}^{(\alpha)}.$$

We have given the intensity  $I_{xy}^y$  at  $\theta = \pi/2$ , inasmuch as the contribution of fluctuations of scalar vari-

ables of the type of density and temperature enter into it at other scattering angles.

The spectral intensities of the fluctuations  $X_\alpha$ ,  $\zeta_{12}^{(\alpha)}$  and  $\Phi_\alpha$  can be found with the help of the fluctuation-dissipation theorem. For this purpose, it is necessary to write down the entire set of hydrodynamic equations with imposed external forces. According to [5,7], this set divides into an equation for  $X_\alpha$

$$4\eta_\alpha \left( \dot{X}_\alpha + \frac{1}{\tau_\alpha} X_\alpha \right) = \Psi_X^{(\alpha)}, \quad \alpha=1, 2, \quad (3)$$

a set of equations for  $\zeta_{12}^{(\alpha)}$  and  $u_2$  ( $u_2$  is the component of the displacement vector)

$$4\eta_\alpha \left( \dot{\zeta}_{12}^{(\alpha)} + \frac{1}{\tau_\alpha} \zeta_{12}^{(\alpha)} \right) - 2\eta_\alpha \frac{\partial \dot{u}_2}{\partial x_1} = \Psi_{12}^{(\alpha)}, \quad \alpha=1, 2, \quad (4)$$

$$\rho \ddot{u}_2 - 2 \left( \mu_1 \frac{\partial \zeta_{12}^{(1)}}{\partial x_1} + \mu_2 \frac{\partial \zeta_{12}^{(2)}}{\partial x_1} \right) = F_2 - \frac{1}{2} \left( \frac{\partial \Psi_{12}^{(1)}}{\partial x_1} + \frac{\partial \Psi_{12}^{(2)}}{\partial x_1} \right)$$

and, finally, a set of equations for  $\Phi_\alpha$  and  $U_1$ ,

$$3\eta_\alpha \left( \dot{\Phi}_\alpha + \frac{1}{\tau_\alpha} \Phi_\alpha \right) - 2\eta_\alpha \frac{\partial \dot{u}_1}{\partial x_1} = \Psi_\Phi^{(\alpha)}, \quad \alpha=1, 2, \quad (5)$$

$$\rho \ddot{u}_1 - \left( \tilde{K}_T + \frac{i\omega T \tilde{P}_T}{i\omega \tilde{c}_V + k^2 \kappa} \right) \frac{\partial^2 u_1}{\partial x_1^2} - 2 \left( \mu_1 \frac{\partial \Phi_1}{\partial x_1} + \mu_2 \frac{\partial \Phi_2}{\partial x_1} \right) = F_1 - \frac{2}{3} \left( \frac{\partial \Psi_\Phi^{(1)}}{\partial x_1} + \frac{\partial \Psi_\Phi^{(2)}}{\partial x_1} \right).$$

Here  $\eta_1$  and  $\eta_2$  are the contributions of two relaxation processes to the coefficient of shear viscosity at zero frequency (the total viscosity is  $\eta = \eta_1 + \eta_2$ );  $\mu_1$  and  $\mu_2$  are their contributions to the instantaneous shear modulus,  $\Psi_X$ ,  $\Psi_{12}$ ,  $\Psi_\Phi$  and  $F_i$  are the external forces conjugate with  $X$ ,  $\zeta_{12}$ ,  $\Phi$  and  $u_i$ ;  $\tilde{K}_T$  is the isothermal elastic modulus,  $\tilde{P}_T$  is the temperature coefficient of the pressure,  $\tilde{c}_V$  is the specific heat, and  $\kappa$  is the coefficient of thermal conductivity. The tilde  $\sim$  indicates that the thermodynamic coefficients are complex (for harmonic processes) and can have dispersion if there are scalar relaxation variables in the set. If, as is usually the case, the dispersion is small, then, in the study of anisotropic scattering, its detailed shape is unimportant and it suffices to consider only the existence of bulk viscosity.

Applying the fluctuation-dissipation theorem to Eqs. (3) and (4), we get

$$\langle X_\alpha^2 \rangle_{\omega k} = \frac{k_B T}{(2\pi)^4} \frac{\eta_\alpha}{2(\mu_\alpha^2 + \omega^2 \eta_\alpha^2)}, \quad \alpha=1, 2,$$

$$\langle \zeta_{12}^{(1)2} \rangle_{\omega k} = \frac{k_B T}{(2\pi)^4} \frac{\tau_1}{2\mu_1 \Delta} [(\omega^2 \tau_2 - \Omega_2)^2 + (\omega^2 + \Omega_1 \Omega_2)],$$

$$\langle \zeta_{12}^{(2)2} \rangle_{\omega k} = \frac{k_B T}{(2\pi)^4} \frac{\tau_2}{2\mu_2 \Delta} [(\omega^2 \tau_1 - \Omega_1)^2 + (\omega^2 + \Omega_1 \Omega_2)], \quad (6)$$

$$\langle \zeta_{12}^{(1)} \zeta_{12}^{(2)} \rangle_{\omega k} = \frac{k_B T}{(2\pi)^4} \frac{\Omega_2 \tau_1}{2\mu_2 \Delta} [\omega^2 (\tau_1 + \tau_2) - (\Omega_1 + \Omega_2)],$$

where

$$\Delta = [\omega^2 (\tau_1 + \tau_2) - (\Omega_1 + \Omega_2)]^2 + \omega^2 [\omega^2 \tau_1 \tau_2 - 1 - (\Omega_1 \tau_2 + \Omega_2 \tau_1)]^2,$$

$$\tau_\alpha = \eta_\alpha / \mu_\alpha, \quad \Omega_\alpha = k^2 \eta_\alpha / \rho, \quad \rho - \text{density}.$$

In the range of low frequencies  $\omega < 1/\tau_1$  (for definiteness, we assume that  $\tau_2 < \tau_1$ ) the intensity  $I_{xy}^y$  is represented in the form

$$I_{xy}^y \sim \frac{A_1^2 \tau_1}{\mu_1} + \frac{A_2^2 \tau_2}{\mu_2} - \frac{k^4 \eta}{\rho^2} \frac{(A_1 \tau_1 + A_2 \tau_2)^2}{\omega^2 + (\Omega_1 + \Omega_2)^2} \cos^2 \frac{\theta}{2}. \quad (7)$$

It follows from this formula that at  $1/\tau_1 \gg k^2 \eta / \rho$  there is a dip at the center of the line; this dip has a Lorentzian contour with characteristic time  $\rho / k^2 \eta$ .

From Eq. (5), we get

$$\langle \Phi_\alpha \Phi_\beta \rangle_{\omega k} = -\frac{k_B T}{(2\pi)^4} \frac{1}{i\omega} \left[ \frac{1}{3(\mu_\alpha + i\omega\eta_\alpha)} \delta_{\alpha\beta} + \frac{4}{9} \frac{i\omega\eta_\alpha}{(\mu_\alpha + i\omega\eta_\alpha)} \frac{i\omega\eta_\beta}{(\mu_\beta + i\omega\eta_\beta)} \frac{k^2}{(-\rho\omega^2 + k^2 R)} - \kappa, c_1 \right], \quad (8)$$

where

$$\tilde{R} = \tilde{R}_T + \frac{i\omega T \tilde{p}_T^2}{i\omega \tilde{c}_v + k^2 \kappa} + \frac{4}{3} i\omega \left( \frac{\eta_1}{1+i\omega\tau_1} + \frac{\eta_2}{1+i\omega\tau_2} \right).$$

As was shown previously,<sup>[7]</sup> the contribution of the second term in the correlators  $\langle \Phi_\alpha \Phi_\beta \rangle_{\omega k}$  can be significant only in the immediate vicinity of the Mandel'shtam-Brillouin frequency  $\Omega_B$ , while its integrated intensity is small and depends on the relation between  $1/\tau_1, 1/\tau_2$  and  $\Omega_B$ . Thus, for example (see<sup>[17]</sup>), if  $1/\tau_1 \ll \Omega_B \ll 1/\tau_2$ , then  $\langle \Phi_1 \Phi_2 \rangle_{\omega k} = 0$ , only the contour  $\tau_2$  makes a contribution to  $\langle \Omega_2^2 \rangle_{\omega k}$ , and the contour of  $\langle \Phi_1^2 \rangle_{\omega k}$  is determined by the sum of the contributions of the contours  $\tau_1$  and  $\Omega_B$ . Here the integrated contribution of the contour  $J_{\Omega_B} = (\frac{4}{9}) [KS(\Omega_B) + (\frac{4}{3})\mu_1]^{-1}$  is much less than the contribution of the contour  $J_{\tau_1} = (\frac{1}{3})\mu_1 - (\frac{4}{9}) [KS(\Omega_B) + (\frac{4}{3})\mu_1]^{-1}$ .

As is seen from Eqs. (1) and (6), for a quantitative comparison of theory with experiment it is necessary to know six parameters:  $A_1, A_2, \eta_1, \eta_2, \mu_1$  and  $\mu_2$ , which can be calculated from six experimentally measured quantities.

A large part of the information is obtained from analysis of the spectra of scattered light, and a small amount from other experiments. As the latter, we used the determination of the Maxwell constant from an experiment on the double refraction in flow and measurement of shear viscosity with the help of an Ostwald viscosimeter.

Using the obtained experimental data, we can construct a set of algebraic equations for the determination of all the necessary parameters. In accord with Eqs. (2), (6) and (8), if we neglect the contribution of the Mandel'shtam-Brillouin components, the ratio of the integrated intensities of the narrow and wide contours in the  $I_{xy}^z$  component is equal to  $(A_1^2/\mu_1)/(A_2^2/\mu_2)$  and the relative depth of the central dip in the  $I_{xy}^z$  component at  $\theta = \pi/2$  is, in accord with (7),  $(M^2/\eta)(2A_1^2\tau_1/\mu_1)$ , where  $M = A_1\tau_1 + A_2\tau_2$  is the Maxwell constant. Then the set of equations takes the form

$$\begin{aligned} \eta_1 + \eta_2 &= C_1, & \frac{A_1^2/\mu_1}{A_2^2/\mu_2} &= C_2, \\ M &= A_1\tau_1 + A_2\tau_2 = C_3, & \frac{M^2/\eta}{2A_1^2\tau_1/\mu_1} &= C_4, \\ \tau_1 &= \eta_1/\mu_1 = C_5, & \tau_2 &= \eta_2/\mu_2 = C_6. \end{aligned} \quad (9)$$

The complete set of experimentally measured quantities  $C_1, \dots, C_6$  was determined only for the temperature of 11°C (see Table II). The sole exception is the Maxwell constant  $M$ , which was measured at 22°C. Its value was converted to 11°C under the assumption that  $M \sim \eta/T$ . Possible deviations from this dependence in such a small temperature range are much less than the errors of measurement of  $M$  (~10%). The data obtained from the spectra  $I_{xy}^z$  and  $I_{xy}^y$  ( $\theta = \pi/2$ ) and used in subsequent calculations are shown in Table II. The set (9) is easily solved relative to the unknowns  $A_1, A_2, \eta_1, \eta_2, \mu_1$  and  $\mu_2$ . It has two solutions, which differ by the sign of the ratio  $A_1/A_2$ . The values of the param-

TABLE II

$t, ^\circ\text{C}$	$C_1 = \eta_1 + \eta_2$ 10 <sup>-2</sup> poise	$C_2$	$C_3 = M$ 10 <sup>11</sup> sec	$C_4$	$C_5 = \tau_1$ 10 <sup>11</sup> sec	$C_6 = \tau_2$ 10 <sup>-12</sup> sec
11	5	3	(17.3)	0.38	5.6	0.46
22	3.7	2.75	12.3	0.35	3.9	—
49	2.02	2.40	—	0.30	2.3	—

TABLE III

$t, ^\circ\text{C}$	sign of $A_1/A_2$	$\eta_1$ 10 <sup>-2</sup> Poise	$\eta_2$ 10 <sup>-2</sup> Poise	$\mu_1$ dyne/cm <sup>2</sup>	$\mu_2$ dyne/cm <sup>2</sup>	$A_1$	$A_2$
11	>0	3.55	1.45	0.64	3.15	0.30	1.32
11	<0	4.00	1.00	0.71	2.15	0.32	-1.0
22	>0	2.35	1.35	0.60	—	—	—
49	>0	1.05	1.00	0.46	—	—	—

eters for both solutions are shown in the first two columns of Table III.

Comparison of the theoretical and experimental spectra is given in Figs. 7 and 8. Both equivalent sets of parameters give, of course, the same theoretical spectra; for definiteness we use the solution with  $A_1/A_2 > 0$ . For comparison with experiment, the function  $I_{xy}^z(\omega)$  calculated from Eqs. (1) and (6), is convoluted with the apparatus function of the optical system  $K(\omega)$ :

$$\hat{I}_{xy}^z(\omega) = \int_{-\infty}^{\infty} K(\omega - \omega') I_{xy}^z(\omega') d\omega'.$$

The shape of the apparatus function for the two lasers used is shown in Figs. 4a and 4b. Figure 7a shows the scattering spectra obtained at different angles with the narrow apparatus function, and Fig. 7b, with the broad one. The theoretical values are plotted as circles on the experimental spectrum. For comparison, the ordinate scale was so chosen that the maximum values of both curves were the same. As seen from the figures, the shapes of the curves and the locations of the maxima are approximately identical, with the exception of the central points  $\omega = 0$ . These points do not coincide partly because of the inaccuracy in the determination of the relative depth of the dip, and partly because of the inertia of the recording instrument. The comparison was made only up to frequencies  $\omega \approx 1/\tau_1$ , inasmuch as the divergence associated with overlap of the spectra begins beyond that region. The values of the parameters are very sensitive to the accuracy of determination of the relative depth of the dip  $C_4$ . For illustration, we have marked on Fig. 7a (curve 2) several points of the theoretical curve (triangles) plotted for  $C_4 = 0.25$ . Although the curve itself does not change much at the center, the values of all the found parameters change significantly (for example,  $\eta_1$  becomes equal to  $1.8 \times 10^{-2}$  instead of  $3.6 \times 10^{-6}$  poise,  $\eta_1 = 0.3 \times 10^9$  dyne/cm<sup>2</sup> instead of  $0.62 \times 10^9$  dyne/cm<sup>2</sup>, and so on). Thus,  $C_4$  must be measured with special care, for which purpose it is important to have a very narrow apparatus function.

Figure 8 gives the dependence of  $\nu_{\max}$  on the scattering angle, found from the theoretically calculated spectra convoluted with the narrow and broad apparatus functions (curves 1 and 2). The corresponding experimental values of  $\nu_{\max}$  are shown by triangles and crosses. The significant discrepancy between theory and experiment in the case of a broad apparatus function is due to the difficulty of experimental estimate of  $\nu_{\max}$ , about which we spoke earlier.

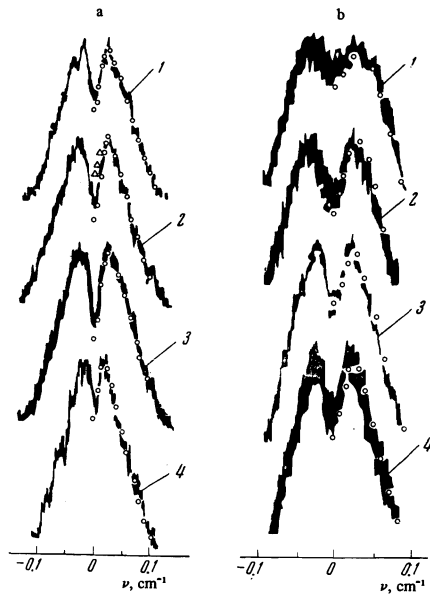


FIG. 7. a – angular dependence of the spectrum of the  $I_{xy}^2$  component for the narrow apparatus function: 1 –  $90^\circ$ ; 2 –  $75^\circ$ ; 3 –  $60^\circ$ ; 4 –  $30^\circ$ ; b – the same for the broad apparatus function: 1 –  $120^\circ$ ; 2 –  $90^\circ$ ; 3 –  $60^\circ$ ; 4 –  $45^\circ$ . The circles indicate theoretical values.

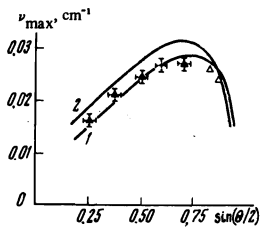


FIG. 8. Angular dependence of  $\nu_{\max}$ . 1 – theoretical curve for the narrow apparatus function; 2 – theoretical curve for the broad apparatus function; experimental values are shown by crosses and triangles, respectively.

We note that the location of the frequency of the maximum at low viscosities depends weakly on the relative depth of the dip. Actually, it follows from Eqs. (1) and (6) that when  $1/\tau_2 \gg 1/\tau_1 \gg k^2\eta/\rho$  in the frequency range  $\omega \ll 1/\tau_2$ , the result of Keyes and Kivelson is obtained.<sup>[9]</sup>

$$I_{xy}^2(\omega) \approx \frac{J_1}{\omega^2 + \omega_1^2} - \frac{J_2}{\omega^2 + \omega_2^2}, \quad (10)$$

where  $\omega_1 = 1/\tau_1$ ,  $\omega_2 = k^2\eta/\rho$ . The function  $I_{xy}^2(\omega)$  has a maximum at  $\omega = D^{1/4} \sqrt{\omega_1 \omega_2}$ , where  $D$  is the relative depth of the dip and is equal to

$$D = \left( \frac{J_2}{\omega_2^2} \right) / \left( \frac{J_1}{\omega_1^2} \right).$$

We note that neglect of the contour  $J_{\Omega B}$  in the contribution in the calculation of the ratio of the integrated intensities is justified. Inasmuch as  $K_S \sim 2.5 \times 10^{10}$  dyne/cm<sup>2</sup>, it follows as is seen from Table III, that this contribution is about 1/30th the contribution of the contour  $L_1$ .

One could have assumed a priori that the anisotropy is determined by the shear stress, as in a simple Maxwell liquid. In this case, we would have had

$$\delta \epsilon_{ik} \sim \sigma_{ik} = 2\mu_1 \zeta_{ik}^{(1)} + 2\mu_2 \zeta_{ik}^{(2)}.$$

Comparing with the formula  $\delta \epsilon_{ik} = A_1 \zeta_{ik}^{(1)} + A_2 \zeta_{ik}^{(2)}$ , we see that  $A_1/\mu_1 = A_2/\mu_2$ . The experimental values of these ratios differ by almost an order of magnitude; consequently, the anisotropic scattering is not described as scattering from stress fluctuations.

By calculating the Maxwell constant from the found values of  $A_1$ ,  $A_2$ ,  $\mu_1$  and  $\mu_2$ , it can be established that this constant is practically entirely due to the changes of  $\zeta^{(1)}$  and a more rapid process makes almost no contribution to the dynamic double refraction at low frequencies. The effect of  $\zeta^{(2)}$  on the light scattering is significant—the integrated intensity of the broad contour amounts to  $1/3$  of the intensity of the narrow one. However, at the observed ratio of the characteristic times  $\tau_1$  and  $\tau_2$  the parameters of the high-frequency process have practically no effect on the shape of the central part of the spectrum. To check on this statement, the values of  $C_8 = \tau_2$  were varied from 0 to  $1.5 \times 10^{-12}$  sec; the shape of the central part of the calculated spectrum was virtually unchanged and the parameters  $\mu_1$ ,  $\eta_1$  and  $A_1$  changed by not more than 5%, i.e., within the limits of error of the experiment. Thus, without exact measurements of  $\tau_2$ , we can find all the parameters of the slow process, and also  $\eta_2$  and  $A_2^2/\mu_2$ , but not  $A_2$  and  $\mu_2$ .

In addition to the detailed investigations at  $11^\circ\text{C}$ , we also studied the light scattering at  $22$  and  $49^\circ\text{C}$ . For these temperatures, measurements of  $\tau_2$  were not carried out, and the Maxwell constant was also not measured at  $49^\circ\text{C}$ ; therefore, it was not possible to calculate all the parameters here. The measured quantities  $C_1$ ,  $C_2$ ,  $C_4$  and  $C_5$  are shown in Table II. These data are sufficient for the unique determination of  $\eta_1$ ,  $\eta_2$  and  $\mu_1$ , if the inequality  $\tau_2 \ll \tau_1$  is preserved. It is seen from Table III that the modulus  $\mu_1$  falls off rather rapidly with increase in temperature; the viscosities  $\eta_1$  and  $\eta_2$  and the relaxation time  $\tau_1$  (Table II) also fall off, and the ratio  $\eta_1/\eta_2$  does not remain constant. From this latter fact we can draw the conclusion that two molecular processes responsible for the observed relaxational phenomena have probably essentially different natures.

Thus, from the results of comparison of theory with experiment, we can conclude that the low-frequency part of the anisotropic scattering spectrum is well described by the hydrodynamic theory.

It is interesting to compare these results with the results of the theory of Volterra.<sup>[18]</sup> Both theories differ only in the form of the rheological equation

$$\sigma_{ik} = 2 \left[ \frac{i\omega\eta_1\mu_1}{\mu_1 + i\omega\eta_1} + \frac{i\omega\eta_2\mu_2}{\mu_2 + i\omega\eta_2} \right] u_{ik}, \quad (11a)$$

$$\sigma_{ik} = 2 \left[ \frac{1}{\mu_\infty} + \frac{1}{\mu_r + i\omega\eta_r} + \frac{1}{i\omega\eta_0} \right]^{-1} u_{ik}. \quad (11b)$$

Comparing Eqs. (11a) and (11b) as well as the expressions for the free energy and for  $\delta \epsilon = A_1 \zeta_1 + A_2 \zeta_2 = A_\infty \zeta_\infty + A_r \zeta_r$ , we have no difficulty in obtaining formulas which connect the parameters of the two models. Thus, the model (11b), which corresponds to the Volterra theory, is expressed in terms of the parameters of our model in the following way:<sup>1)</sup>

$$\begin{aligned} \mu_\infty &= \mu_1 + \mu_2, & \mu_r &= \gamma \frac{\eta_1 + \eta_2}{\tau_1 - \tau_2}, & \eta_0 &= \eta_1 + \eta_2, \\ \eta_r &= \gamma \frac{\mu_1 + \mu_2}{\tau_1 - \tau_2} \tau_1 \tau_2, & \zeta_\infty &= \frac{\mu_1 \zeta_1 + \mu_2 \zeta_2}{\mu_1 + \mu_2}, & \zeta_r &= \frac{1}{\gamma} (\zeta_1 - \zeta_2), \end{aligned}$$

$$A_\infty = A_1 + A_2, \quad A_r = \gamma \frac{A_1 \mu_1 + A_2 \mu_2}{\mu_1 + \mu_2},$$

where

$$\gamma = \frac{\mu_1 + \mu_2}{\mu_1 \mu_2} \frac{\eta_1 + \eta_2}{\tau_1 - \tau_2}.$$

Inasmuch as the two models are purely phenomeno-

TABLE IV

$t, ^\circ\text{C}$	sign of $A_1/A_2$	$\eta_0, 10^{-2}$ poise	$\eta_{T_1}, 10^{-2}$ poise	$\mu_\infty, 10^{10}$ dyne/cm <sup>2</sup>	$\mu_{T_1}, 10^{10}$ dyne/cm <sup>2</sup>	$A_\infty$	$A_T$
11	>0	5	2.1	3.2	1.3	1.50	0.45
11	<0	5	1.3	2.2	1.45	-0.68	0.45
22	>0	3.7	2.4	—	1.5	—	—
49	>0	2.02	1.9	—	1.7	—	—

logical, the attempt to ascribe a definite molecular meaning to the parameters of one of these means the choice of this model as the "more basic." Thus, Volterra starts out from a model in which the deformation is broken up into three independent parts: viscous flow, instantaneous reversible deformation, and delayed reversible deformation. It is assumed that these three parts are functions of the stress. It is assumed further that the delayed part of the deformation is due to the orientation of the molecules, and the instantaneous deformation is not connected with the optical anisotropy ( $A_\infty = 0$ ). We note that Keyes and Kivelson<sup>[9,10]</sup> criticize the Volterra theory because it attributes to orientations the broad but not the narrow contour in the spectrum. This is in an obvious misunderstanding: the variable  $\zeta_T$  makes a contribution to both observed contours.

One can divide the stress into two parts with equal success. These parts are independent of one another and are Maxwellian (i.e., obeying an equation of the form  $\dot{u} = \sigma/\mu + \sigma/\eta$ ) functions of the deformation (model (11a) and consider one of these parts as due to the orientation of the molecules, and the other to their displacement from the instantaneous temporal equilibrium positions. Similarly, we can compare other models and also ascribe a "molecular" meaning to them. It must be kept in mind that (11a) and (11b) are only the simplest models which contain the minimum number of parameters. For example, the free energy in them contains only terms of the form  $\zeta_1^2$  but not  $\zeta_1 \zeta_k$ . The natural variables of molecular theory cannot possess such properties. It is clear that a sound choice between the different possibilities can be made only on the basis of a quantitative theory and any attempt to guess the "true" model from general considerations is scarcely justified.

Inasmuch as the Volterra model is widely used, we have given the parameters of this model in Table IV. They have been computed from our data. Calculations for the temperatures 22 and 49°C are based on an approximation which is valid for  $\tau_2 \ll \tau_1$  and  $\mu_2 \gg \mu_1$ . The assumption of the non-activity of the instantaneous deformation<sup>[18]</sup> is evidently not satisfied,  $A_\infty \neq 0$ . The modulus  $\mu_T$  increases with temperature as Volterra assumed.

In conclusion, we note that in the case of a large difference between  $\mu_1$  and  $\mu_2$  or  $\tau_1$  and  $\tau_2$ , a rough identification of the parameters of the phenomenological and molecular theories is justified, up to a point. Actually, it is not difficult to verify that under this condition one can separate in all models (11) two characteristic times, which are close in order of magnitude to  $\tau_1$  and  $\tau_2$ ; for the model (11b), for example, this is

the time of retardation of the internal variable  $\eta_T/\mu_T$  and the relaxation time of the stress (at fixed  $\zeta_T$ )  $\eta_0/\mu_\infty$ . This allows us to assume that  $\tau_1$  and  $\tau_2$  agree in order of magnitude with the characteristic times of molecular processes. However, such subtle conclusions on the molecular meaning of the temperature dependence of the parameters, for example, must be deduced with caution. Thus, the moduli  $\mu_1$  and  $\mu_T$  in the models (11a) and (11b) are close in magnitude, and one can probably associate them with the same molecular parameter, even though  $\mu_1$  falls off and  $\mu_T$  increases with temperature.

The authors consider it their pleasant duty to thank V. A. Solov'ev for constant interest in the work and useful comments and also S. M. Rytov, V. S. Starunov, and I. L. Fabelinskiĭ for discussion of the results of the research.

<sup>1)</sup>These formulas were obtained by V. A. Solov'ev.

- <sup>1</sup>G. J. Stegeman and B. P. Stoicheff, Phys. Rev. Lett. 21, 202 (1968).  
<sup>2</sup>V. S. Starunov, E. V. Tiganov, and I. L. Fabelinskiĭ, ZhETF Pis. Red. 5, 317 (1967) [JETP Lett. 5, 260 (1967)].  
<sup>3</sup>H. G. Craddock, D. H. Jackson, and J. G. Powles, Mol. Phys. 14, 373 (1968).  
<sup>4</sup>L. A. Zubkov, N. B. Rozhdestvenskaya, and A. S. Khromov, ZhETF Pis. Red. 11, 473 (1970) [JETP Lett. 11, 321 (1970)].  
<sup>5</sup>M. A. Leontovich, J. Phys. USSR 4, 499 (1941).  
<sup>6</sup>S. M. Rytov, Zh. Eksp. Teor. Fiz. 58, 2154 (1970) [Sov. Phys.-JETP 31, 1163 (1970)].  
<sup>7</sup>V. P. Romanov and V. A. Solov'ev, Opt. i spektr. 29, 884 (1970).  
<sup>8</sup>H. Ben-Reuven and N. D. Gershon, J. Chem. Phys. 54, 1049 (1971).  
<sup>9</sup>T. Keyes and D. Kivelson, J. Chem. Phys. 54, 1786 (1971).  
<sup>10</sup>T. Keyes and D. Kivelson, J. de Phys. 33C, 231 (1972).  
<sup>11</sup>N. K. Ailawadi, B. J. Berne, and D. Forster, Phys. Rev. A3, 1472 (1971).  
<sup>12</sup>H. G. Andersen and R. Pecora, J. Chem. Phys. 54, 2584 (1971).  
<sup>13</sup>L. A. Zubkov and N. B. Rozhdestvenskaya, Opt. i spektr. 34, 1015 (1973).  
<sup>14</sup>D. A. Pinnow, S. J. Candau, and T. A. Litovitz, J. Chem. Phys. 49, 247 (1968).  
<sup>15</sup>H. W. Leidecher, Jr., J. T. Lac Macchia, J. Acousr, Soc. Am. 43, 143 (1968).  
<sup>16</sup>E. F. Gross, V. P. Romanov, V. A. Solov'ev, and E. O. Chernysheva, Fiz. Tverd. Tela 11, 3686 (1969) [Sov. Phys.-Solid State 11, 3099 (1970)].  
<sup>17</sup>V. P. Romanov, V. A. Solov'ev, and L. C. Filatova, Opt. i spektr. 34, 539 (1973).  
<sup>18</sup>V. Volterra, Phys. Rev. 180, 156 (1969).

Translated by R. T. Beyer  
183